EXPANSION OF SMECTITE BY HEXADECYLTRIMETHYLAMMONIUM

SEUNG YEOP LEE* AND SOO JIN KIM

School of Earth and Environmental Sciences, Seoul National University, Seoul 151-742, Korea

Abstract—The adsorption of hexadecyltrimethylammonium (HDTMA) in smectite was studied by adsorption isotherms, X-ray diffraction (XRD) and high-resolution transmission electron microscopy (HRTEM). Smectites that had reacted for 48 h with HDTMA cations equivalent to $0.2-3.0$ times the cation exchange capacity (CEC) were converted to HDTMA-exchanged smectites with various *d*-spacings. Study of HDTMA-smectites by HRTEM suggests that the HDTMA adsorption results in interlayer expansion with various *d*-spacings and irregular wavy layer structures. We believe that HDTMA loading beyond the CEC of smectite affects the structure of clay by the additional adsorption of HDTMA-Br$^-$ via hydrophobic bonding. Surfactant orientation probably depends on the quantity of surfactant in the interlayer. Our TEM study shows that the structure of the adsorbed HDTMA layer in the interlayers of smectite depends on the charge distribution and chemical composition of smectite.

Key Words—Adsorption, Hexadecyltrimethylammonium, High-resolution Transmission Electron Microscopy, Interlayers, Smectite, Surfactant.

INTRODUCTION

Clay minerals are generally ineffective sorbents for removing organic pollutants from water. However, it has been shown that the sorptive capabilities of clay minerals for organic contaminants can be improved substantially by replacing naturally-occurring inorganic exchange cations with organic cations (Mortland *et al.*, 1986; Smith *et al.*, 1990). It is known that the much higher affinity of organic cations than inorganic cations for the clay interlayer is partly due to lateral interactions of adsorbed organic cations (cooperative adsorption) (Theng, 1974; Rosen, 1989). The most extensively-studied organic substitutes are quaternary ammonium ions of the form $[R\text{N(CH}_3)_3]^+$, where R is an alkyl or aromatic hydrocarbon. Among the quaternary-ammonium compounds studied, HDTMA is one of the most effective at transforming the sorptive capabilities of clays. If clays are treated with HDTMA, their sorption coefficients for several common organic groundwater contaminants, such as benzene, toluene and xylene, increase by more than two orders of magnitude (Boyd *et al.*, 1988; Lee *et al.*, 1989). In addition, HDTMA-modified clays can remove organic anions from water (Brixie and Boyd, 1994).

The microstructural characteristics of modified clays may play an important role in their sorptive abilities, and HRTEM is a powerful tool to investigate microstructural changes and deformation of clay minerals (Vali and Köster, 1986; Cetin and Huff, 1995). Whereas X-ray or neutron diffraction can be used to characterize the average structure, HRTEM permits the direct observation of microstructural features that result from the transformation of clays to organo-clays.

In this paper, we describe the variation of interlayer spacing and the microstructural characteristics of HDTMA-modified smectite when loaded with different levels of HDTMA. We also aim to understand the configuration of organic molecules on the interlayer surface for each HDTMA loading level.

EXPERIMENTAL

Clay sample

A smectite sample was obtained from the Süd-Chemie Korea Company. The sample contains quartz, a 10 Å phyllosilicate, and some heavy minerals as impurities. The <2 μm fractions of smectite were separated by wet sedimentation. 80 g of smectite were dispersed in 1 L of distilled water and allowed to stand for several hours to allow settling of quartz sand and heavy minerals. Then the clay was saturated with Na cations by washing the clay repeatedly with NaCl solution; this step was performed by shaking 4 g of clay with 200 mL of 0.1 M NaCl solution, centrifuging the suspensions, and decanting the supernatant solutions. This process was repeated three times. The Na-saturated smectite was then washed three to four times with distilled water until the AgNO$_3$ test for chloride was negative. The Na-saturated smectite was subsequently frozen and freeze dried for 36 h with a Labconco Model 77545 freeze-dry system. The cation exchange capacity (CEC) of the smectite was determined by the BaCl$_2$ method (Hendershot and Duquette, 1986).

HDTMA bromide

Hexadecyltrimethylammonium (HDTMA) bromide was obtained from Sigma-Aldrich. The HDTMA molecule consists of a 16-carbon chain tail group attached to a 3-methyl quaternary amine head group with a 1+ charge. Adding together the van der Waals packing radii

* E-mail address of corresponding author:
lsyblue@hanmir.com

for a 3-methyl ammonium head group yields a diameter of 0.694 nm. A fully-extended HDTMA chain length of 3.5 nm can be calculated by adding the effective van der Waals radii for the appropriate number of $-CH_2$ and $-CH_3$ groups (Israelachvili, 1991). A typical carbon chain diameter of 0.4 nm can also be calculated from the packing radii (Israelachvili, 1991).

HDTMA isotherm

A batch equilibration isotherm was determined using 20 mg clay samples weighed into 25 mL centrifuge tubes. Water solutions (10 mL each) containing HDTMA equivalent to 0.01−6 times the CEC were added to these tubes. These suspensions were then shaken for 2 days on a shaker at 200 rpm at 25°C. The mixture was centrifuged to yield a clear supernatant solution (8000 rpm for 20 min) and the HDTMA concentrations were measured using a TOC analyzer (TOC-8L, Yanaco).

HDTMA-smectite preparation

The HDTMA bromide was dissolved in warm distilled water. Na-saturated smectite (0.1 g) samples were placed into a series of 25 mL centrifuge tubes containing different volumes of aqueous HDTMA solutions (4.0 cmol L^{-1}), ranging 0.2−3.0 times the CEC, followed by adding distilled water to bring the total volume to 20 mL. The tubes were shaken on a reciprocating shaker at room temperature for 2 days. The suspensions were centrifuged at 8000 rpm for 20 min at 25°C and the supernatant was decanted. After the treated clay was washed with 20 mL of distilled water, it was frozen and freeze dried for 36 h.

X-ray diffraction

20 g of the HDTMA clays were dispersed ultrasonically in 2 mL of distilled water. Other samples were washed with 5 mL of distilled water and 100% ethanol up to ten times to examine the reversibility (or desorption behavior) of HDTMA cations from the interlayer of clay. The basal spacings of HDTMA-smectites were determined under three different relative humidities (RH) by XRD analysis. The water-saturated clay pellet was smeared onto a glass slide and XRD patterns were recorded under 100% RH. The glass slide was then allowed to equilibrate under room temperature and pressure (~40% RH at 25°C) for 5 days. After XRD patterns of the clays were recorded at 40% RH, the glass slide was then placed over dry P_2O_5 in the desiccator (<5% RH) for 3 days after which the XRD pattern was recorded again. Basal spacings were obtained using CuKα radiation and a Rigaku RAD3-C automated X-ray diffractometer fitted with a theta-compensating slit, a 0.2 mm receiving slit, and a diffracted-beam graphite monochromator.

Electron microscopy

Samples for TEM were prepared by a technique modified from that of Vali and Köster (1986). An outline
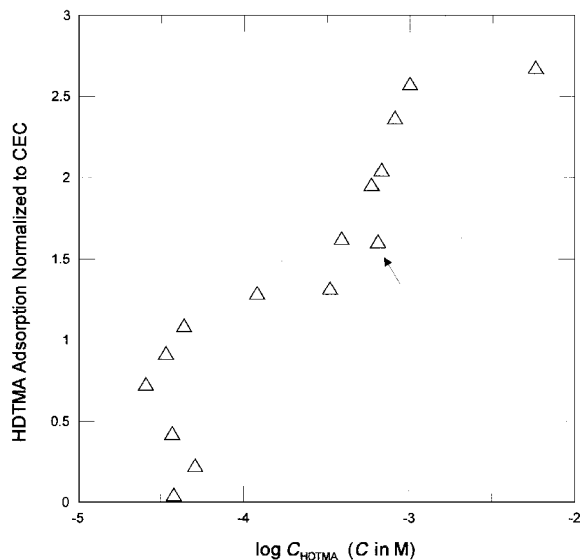

Figure 1. HDTMA adsorption isotherm for the Na^+-saturated smectite.

of the procedure is as follows: 20 mg of HDTMA-smectites were mixed with 1 g of Spurr's resin (obtained by mixing 10 g of resin, 4 g of plasticizer, 26 g of hardener, 0.4 g of accelerator) in a centrifuge tube. The tube was agitated in a rotary mixer for 3 h, then filled with fresh resin after decanting the supernatant. This procedure was repeated twice, and the tube was then placed under vacuum for 30 min. To minimize the possibility of unexpected swelling of organo-clays during the sample treatment, the quantity and volume of the resin exchange and the operation time of the vacuum treatment were limited as much as possible. The clay suspension was added to a capsule mold and fresh resin was poured into the mold. It was left to polymerize in an oven for 24 h at 50°C. The solid polymerized resin block was trimmed, and a pyramidal tip was shaped. Ultrathin sections with a thickness of 50 to 70 nm were then cut from this pyramid-shaped tip by ultramicrotomy. Ultrathin sections were mounted on 300-mesh Cu grids with holey carbon films. In some samples, particles were suspended on a holey carbon film on a 300-mesh Cu grid during ultrasonic dispersal in ethanol. Samples were imaged along the particle edges. The HDTMA-smectite fabrics were examined using the Carl Zeiss EM912Ω and Philips EM420T instruments. Samples were studied at accelerating voltages of 120 and 200 kV.

RESULTS

Adsorption behaviors

The adsorption isotherm of HDTMA by smectite is shown in Figure 1. The total adsorption of HDTMA exceeded 2.5 times the equivalent of the CEC (104.3 cmol/kg) at greater HDTMA loadings. An arrow in Figure 1 indicates an isotherm point (~1.6 CEC) at

which the amount of HDTMA added is equivalent to 2.5 CEC. In fact, some of the HDTMA cations added seemed to remain as micelle in solution, without any interaction with the clay minerals. It means that all HDTMA cations added are not necessarily adsorbed to the smectite from aqueous solution. The isotherm shape of Figure 1 appears as a sigmoidally-shaped curve, which is different from the isotherm curves of non-swelling clays (*e.g.* kaolinite) (Li and Bowman, 1997). Similar experimental isotherm results for swelling clays were reported by Xu and Boyd (1995).

In Figure 2a, the *d*-spacings of wet (water saturated), partially air-dried (dried at ~40% RH) and dry (dried at ≤5% RH) clays were nearly identical at high HDTMA loadings, but differed considerably at low HDTMA loadings (≤1.5 CEC). As the amount of HDTMA added increased from 0.01 to 0.7 CEC (region 1), the d_{001}-spacings of wet clay samples increased from 19.5 to 23.7 Å. No further change in the *d*-spacings was observed from the smectites treated with HDTMA equivalent to 0.8−1.5 times the CEC (region 2). The d_{001}-spacings range from 27.6 to 40.5 Å for the smectites treated with HDTMA equivalent to 1.5−2.5 times the CEC (region 3), but are nearly constant for the smectites treated with HDTMA equivalent to >2.5 CEC (region 4). Partially air-dried clays show considerably reduced d_{001}-spacings compared with wet clays with added HDTMA ≤1.5 CEC. Compared to wet HDTMA clay, the partially air-dried (40% RH) clays exhibit great changes in *d*-spacings (~5 Å) for HDTMA loading ≤1.5 CEC, but only small changes for HDTMA loading >1.5 CEC. The complete drying of the clays (≤5% RH) resulted in further reductions in or nearly the same *d*-spacings for HDTMA loading ≤1.5 CEC. The XRD patterns of wet clays (Figure 2b) show poorly-defined peaks, while partially air-dried (40% RH) clays (Figure 2c) show relatively well-defined peaks with high intensity. The XRD peaks for partially-loaded clays (0.5 and 0.8 CEC) were broadened in comparison to clays with other loading levels (Figure 2c). It seems that the slight variations in *d*-values at structural transitions (*i.e.* monolayer to bilayer or pseudotrimolecular layer) contribute directly to increased peak widths.

Desorption behaviors

Desorption of HDTMA was also studied in order to understand the interaction of alkyl chains of HDTMA in the interlayer region of smectite. The desorbability of the adsorbed HDTMA depended on the HDTMA loading level (Figure 3). The *d*-spacings changed substantially (from 37.1 to 29.2 Å at the smectite treated with HDTMA equivalent to 2.0 times the CEC) on the fifth water wash at 100% RH, but only slightly (from 40.5 to 37.7 Å at the smectite treated with HDTMA equivalent to 3.0 times the CEC) (Figure 3a). On the tenth water wash (100% RH), the *d*-spacing for samples at 3.0 CEC greatly decreased, eventually reaching 26.8 Å.

Desorption of HDTMA by ethanol shows a somewhat different behavior from that by water in the variation of *d*-spacing. The d_{001}-spacing of ~22 Å for HDTMA-smectite at 0.5 CEC changed to ~15 Å, whereas the interlayer spacing for the water-washed sample did not change appreciably (Figure 3a). The larger decrease in the interlayer spacing of HDTMA-smectite following the ethanol wash might be due to the evaporation of ethanol, which causes the interlayer of clay to be significantly less hydrous. The smectites treated with HDTMA equivalent to 2.0 and 3.0 times the CEC show spacings of ~26 and 30 Å at 100% RH, respectively, by the tenth enthanol wash, suggesting some HDTMA resistance to desorption. However, the XRD peak intensities of these samples are very weak (arrows in Figure 3c), indicating that only a small fraction of the alkyl chains exist in a paraffin-type arrangement in the wet state. Under completely dry conditions (≤5% RH), the d_{001}-spacing reduced to ~19.5 Å (Figure 3d).

At 5% RH (Figure 3b), the HDTMA-smectites loaded with <1.0 CEC show similar *d*-spacings, regardless of the numbers and kinds of washes, while those treated to >2.0 CEC show characteristic features. The smectite treated with HDTMA equivalent to 2.0 times the CEC exhibited a *d*-spacing of 22.0 Å at the fifth water wash, indicating a pseudotrimolecular layer, whereas the sample treated with HDTMA equivalent to 3.0 times the CEC showed a *d*-spacing of 40.1 Å by the fifth water wash, suggesting a paraffin-type structure. According to Lagaly (1994), the pseudotrimolecular layer consists of three alkyl chains in which the unpolar chain ends are shifted one above the other by the formation of kinks. In contrast, the chains in 'all-*trans*' conformation, point away from the surface in paraffin-type structures. The smectites treated with HDTMA equivalent to 3.0 times the CEC show nearly the same *d*-spacings (~40 Å) from zero to fifth water wash. This behavior suggests that the high adsorption of cationic molecules on clay in excess of the CEC (*e.g.* >1.0 CEC) is due to the great binding energy of the quaternary cations (Zhang *et al.*, 1993).

TEM results

Ultramicrotome sections perpendicular to the 00*l* plane of untreated smectite show compact and continuous silicate layers (Figure 4). Most layers show a spacing of 12 Å, with values of ~10 Å in places, presumably due to partial collapse upon loss of water in the vacuum of the TEM (Ahn and Peacor, 1986). However, they could also be interpreted as local heterogeneities in the original chemistry and/or struture (Lee and Peacor, 1986).

Figure 5 shows lattice fringes after treatment with HDTMA ions equivalent to 0.2 times the CEC of the smectite. We were able to obtain an SAED pattern (insert, Figure 5), where the 14 Å basal reflection was confirmed. However, the lattice fringes show some wavy structure in areas. It seems that as Na ions in the
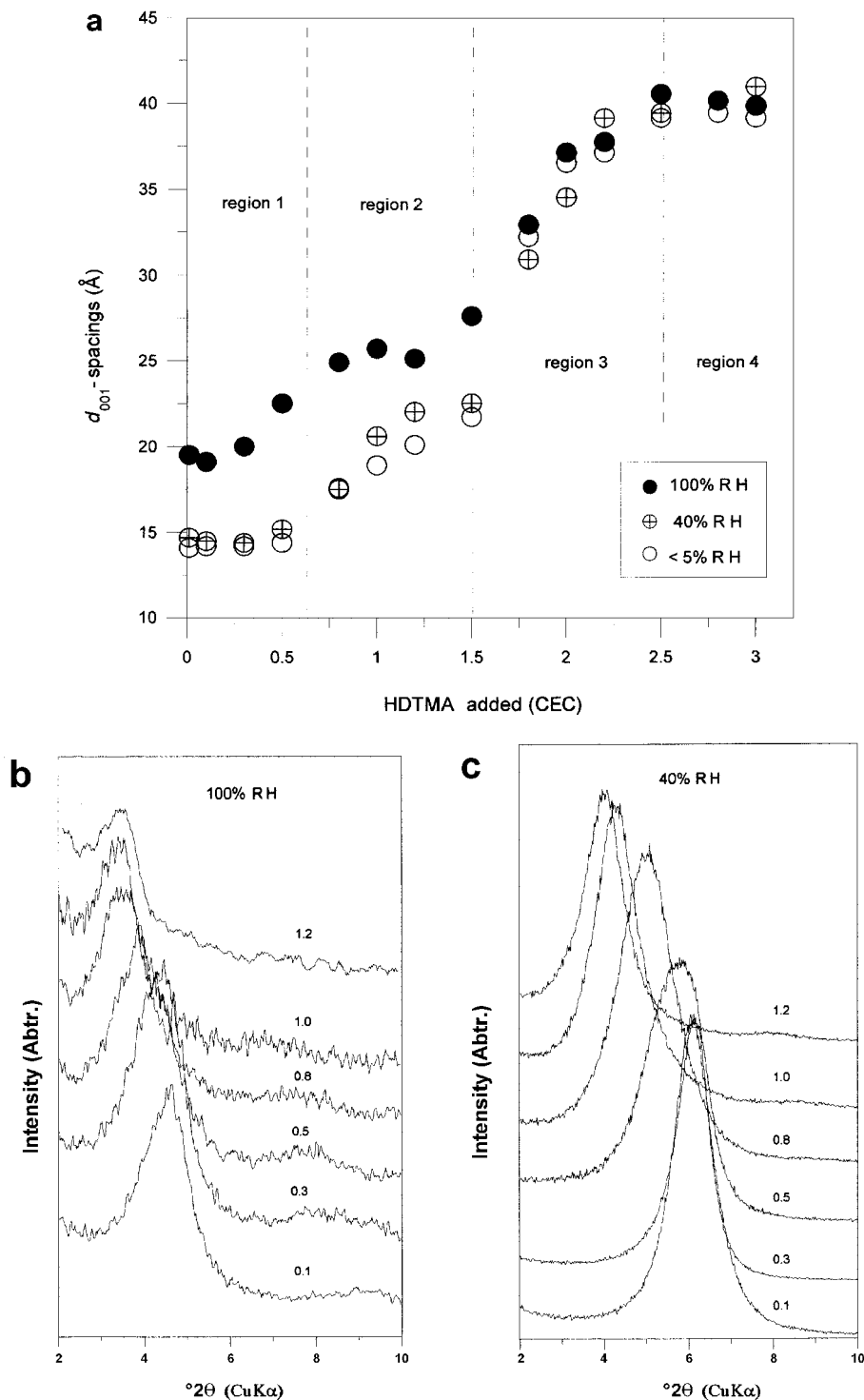
Figure 2. Plots of HDTMA added *vs.* d_{001}-spacings (a) of HDTMA-smectites and their selected XRD patterns (b and c) at different relative humidities (RH). The numbers on the XRD curves (b and c) indicate the HDTMA loadings normalized to CEC.

interlayer of smectite are replaced by HDTMA cations, different interlayer spacings result (Figure 6). The ultrathin section (Figure 6) reveals an overall 17 Å (nearly double layer) spacing, but partial 14 Å (mono-

layer) and/or 21 Å (pseudotrimolecular layer) spacings are also observed.

As HDTMA loading increases, TEM micrographs show poorly-defined broad fringes varying from 17 to
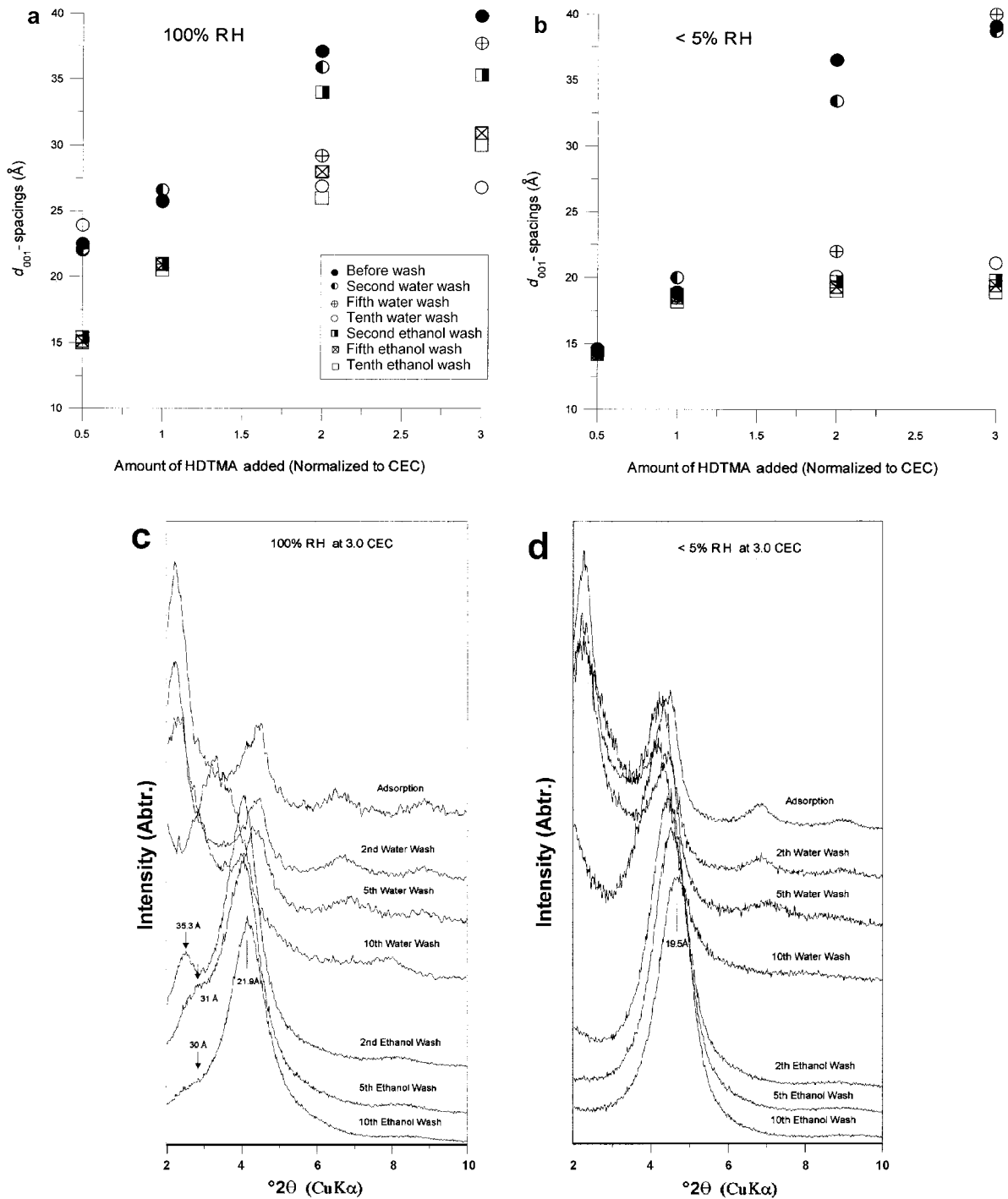
Figure 3. Desorption of HDTMA by water or ethanol wash from HDTMA-smectites and their selected XRD patterns (c and d) at two different relative humidities (100 and <5% RH). Note the reduction of d-spacings due to desorption of HDTMA cations by water or ethanol wash, and the high reduction of d-spacings by ethanol wash compared to water wash.

24 Å in thickness (Figure 7). The wavy, anastomosing and discontinuous lattice-fringe images exhibit a large number of edge dislocations and changes in image contrast along the layers. These defects are due to small orientation changes in the crystal (Banfield and Eggleton, 1988).

Figure 8a shows the layer structure of smectite after HDTMA treatment corresponding to 2.0 times the CEC. Some lattice fringes are distorted or wavy over several hundreds of angstroms. They generally reveal layer spacings of 25–30 Å, which are somewhat lower than the values obtained by XRD. Such a difference in layer
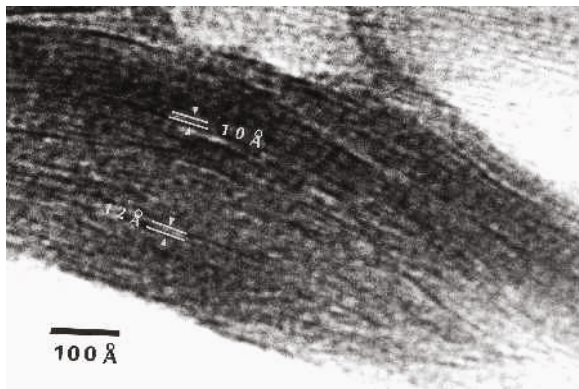
Figure 4. Lattice fringe image of the untreated and resin-embedded smectite showing layer spacings of 10−12 Å. The layer thickness is not uniform.

Figure 5. Ultrathin section of smectite treated with HDTMA ions equivalent to 0.2 times the CEC of the clay. Average value of $d_{001} = 14$ Å is displayed by lattice fringe image and selected area electron diffraction pattern (insert). Note irregular or wavy layer structures (open arrows).

spacing might be due to the sample preparation process for TEM (*e.g.* some HDTMA could be expelled from the clay interlayer during the resin treatment) or to the collapse of layers during TEM observations. Dispersed particles of smectite were examined after treatment with HDTMA equivalent to 2.0 times the CEC (Figure 8b). Like the sample prepared by embedding and ultramicrotomy, the layer spacings averaged 27−28 Å and
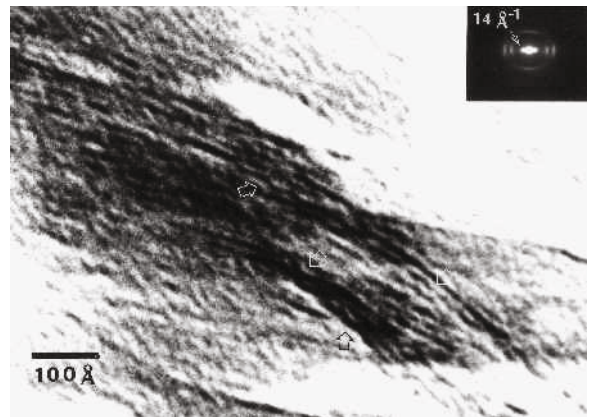
exhibited wavy or curved layers with variable thickness (Figure 8b).

The HDTMA-smectite that was treated with more than 2.5 times the CEC (*i.e.* the plateau of the HDTMA adsorption isotherm) shows non-parallel and slightly curved fringes of ~30−33 Å, similar to those treated

Figure 6. Ultrathin section of smectite treated with HDTMA ions equivalent to 0.8 times the CEC of the clay. The overall layer spacing is 17 Å, and is slightly curved, but spacings smaller or larger than 17 Å are observed. 14 Å (thin arrows) and 21 Å (open arrows) layer spacings are shown.
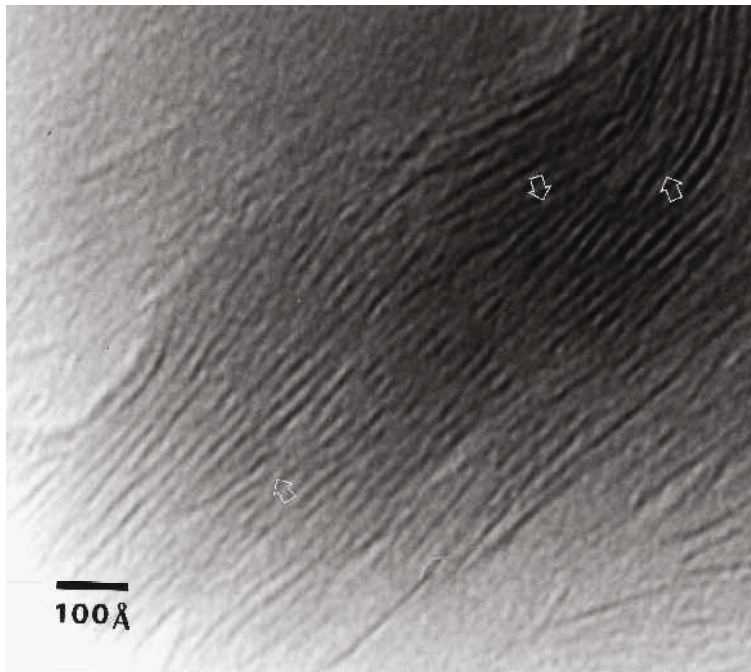
Figure 7. HRTEM images of HDTMA-smectite (1.0 CEC) in ultrathin section. Lattice fringes show expanded and wavy layers with various spacings from 17−24 Å. Edge dislocations are indicated by arrows.

with 2.0 times the CEC but slightly more expanded. Such layer variation may reflect heterogeneity in composition or it may be an artifact of the changing orientation of layers relative to the beam (Guthrie and Veblen, 1990). Furthermore, some researchers have suggested that montmorillonite swells in parts from the
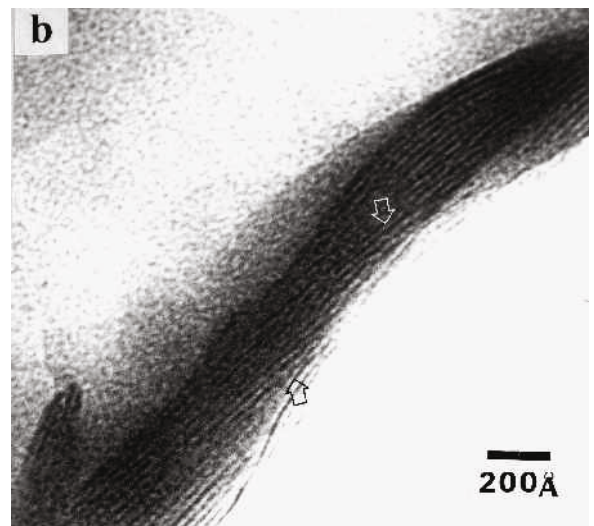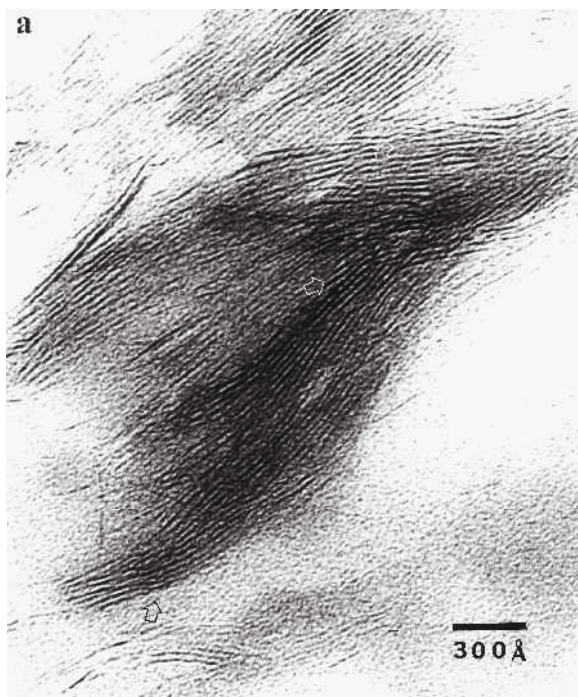

Figure 8. HRTEM images of HDTMA-smectite (2.0 CEC) in ultrathin section. (a) Slightly curved basal spacing of 25−30 Å; (b) expanded basal spacing of 27−28 Å in dispersed particle. Wavy or curved layer structures are shown by arrows.
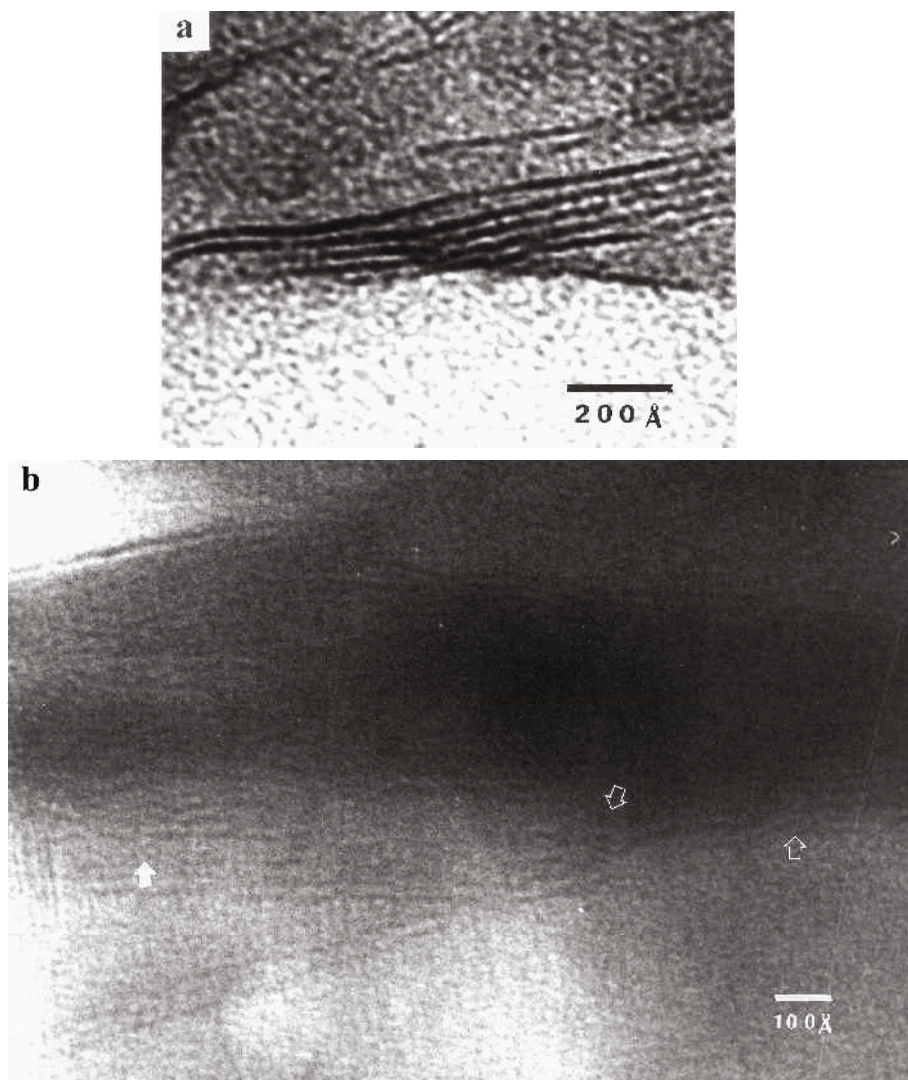
Figure 9. HRTEM image of HDTMA-smectite at ~2.5 CEC: (a) ultrathin section showing layer spacing of 30−33 Å; (b) dispersed particle with layer spacing of ~30 Å. Wavy or crumpled layer structures are seen (arrows).

embedding resin (Vali and Köster, 1986; Marcks *et al.*, 1989). However, our study shows that the basal spacing (~30 Å) of dispersed particles of HDTMA-smectite (Figure 9b) is not distinguishable from that of the resin-embedded HDTMA-smectite (Figure 9a).

DISCUSSION

The curve of the HDTMA adsorption isotherm (Figure 1) shows that the sorption behaviors of cationic surfactants by smectite are stepwise. The isotherm had a low HDTMA sorption initially but increased dramatically to a maximum around 0.7 CEC, showing the lowest equilibrium HDTMA concentration (*i.e.* log C_{HDTMA} = −4.6). This indicates that the cation exchange of HDTMA for Na in interlayers is not easy at an early stage due to the difficulty in prising open the layers by

very large HDTMA cations. However, the interlayers, once opened, may be very suitable to adsorb HDTMA cations from aqueous solution. As HDTMA adsorption on smectite increases, most intercalation of HDTMA into the layers seems to occur near ~1.6 CEC (arrow in Figure 1), as shown by the d_{001}-spacing in Figure 2a (*i.e.* fully-expanded layers (~40 Å) at ~2.5 CEC). As previously mentioned in the Results section, among the HDTMA cations added in aqueous solution, some HDTMA cations seem to just remain as micelle without any interaction with clay surfaces. In our adsorption isotherm experiment, when HDTMA is added up to an equivalent of 2.5 times the CEC of smectite, the amount adsorbed on the clay surface was ~1.6 CEC (Figure 1), and the amount of added HDTMA (*i.e.* ~2.5 CEC) was the maximum concentration that could be intercalated into the silicate layers (Figure 2a). As HDTMA loadings

continue, an additional sorption of HDTMA by smectite occurs, forming a dramatic slope curve in the isotherm (Figure 1). The additional sorption of HDTMA probably occurs on external rather than internal surfaces of smectite due to the limitation of HDTMA intercalation as mentioned above.

Figure 2a shows the increase of interlayer spacings measured using XRD during HDTMA loading. The stepwise change in d-spacings for dry smectite with increasing HDTMA loading demonstrates the existence of different specific arrangements of HDTMA in the interlayers of smectite (Lagaly and Weiss, 1969) (Figure 2). The thickness of a smectite platelet is 9.6 Å and the height of a flat-lying alkyl chain in the clay interlayers can be 4 or 4.5 Å, depending on its orientation (Brindley and Hoffmann, 1962). The d_{001}-spacings of ~14 Å at the added HDTMA $\leqslant 0.5$ CEC (Figure 2) suggests a monolayer arrangement. Increasing the added HDTMA from 0.5 to 1.5 CEC produces a bilayer arrangement (17−18 Å) or a pseudotrimolecular layer (~22 Å). The smectite treated with HDTMA beyond 1.5 times the CEC results in a paraffin complex (>22 Å). Comparison of the d-spacings of dry clays and partially dry or water-saturated samples reveals that drying alters the interlayer arrangement of HDTMA at $\leqslant 1.5$ CEC. Therefore, structures deduced from dried clay samples do not accurately represent those in aqueous solution and have little relevance to the HDTMA-clay complexes under ambient environmental

conditions (Xu and Boyd, 1995). Although a monolayer is indicated in the dried samples, it does not form in solution even at very low HDTMA loadings (Figure 2). The d-spacings of wet HDTMA-smectite are never <19.1 Å, greater than expected for a densely-packed monolayer or bilayer, indicating very loose and probably less-ordered arrangements in the wet state. A disordered liquid-like arrangement of chains may be preferred in the water-saturated interlayers (Xu and Boyd, 1995). In this disordered arrangement the chains may not remain flat, but instead overlap and co-mingle with HDTMA ions on the opposite sides of the interlayers.

Transmission electron microscopy permits direct observation of microstructural distortions generated by the configurations of organic molecules on the interlayer surface. Lattice fringes of smectites after treatment with HDTMA ions equivalent to 0.2 times the CEC of smectite show some wavy structure in parts (Figure 5), which is interpreted as the response to stress that is generated from intercalation of organic cations. According to a predictive model of Laird (1994), there is an elastic or labile deformation of silicate layers of smectite due to the configuration of surfactant, resulting in a form of 'island-like' structure. There is a possibility that the stresses caused by intercalation of organic cations will deform the original texture of the clay.

Depending on the HDTMA concentrations reacted with smectite (*e.g.* $\geqslant 0.8$ CEC), there occur differential layer expansions (Figures 6−9) which are variable even
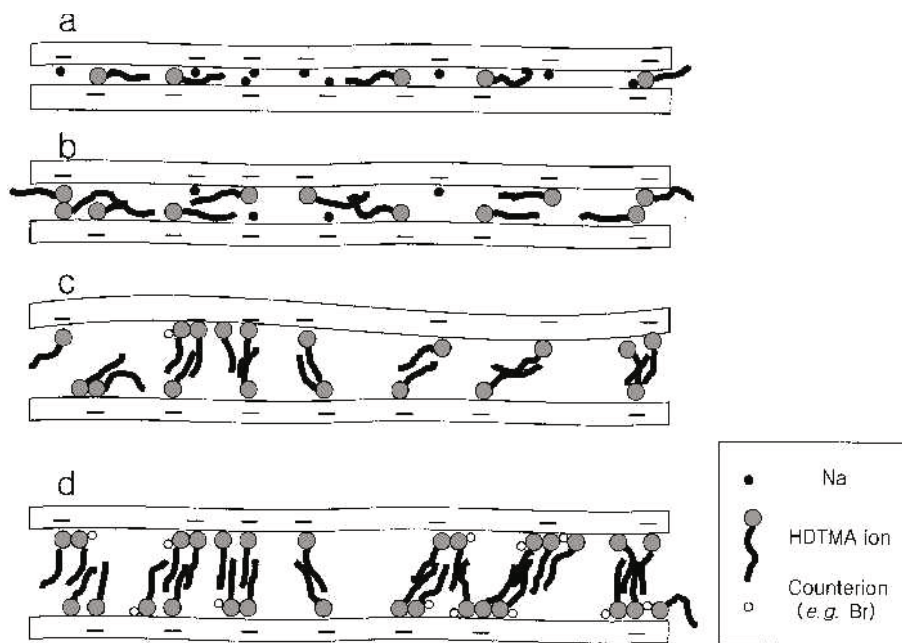

Figure 10. A schematic model for a possible configuration of HDTMA ions in interlayers with heterogeneous charge distribution at each swelling stage in solution: (a) initial stage of HDTMA intercalation (0.1−0.7 CEC); (b) exchange of most Na$^+$ by HDTMA (0.7−1.0 CEC); (c) vertical rearrangement of HDTMA (1.0−1.5 CEC); (d) continuous hydrophobic adsorption of HDTMA ($\geqslant 1.5$ CEC).

within layers (Figure 7). This observation clearly shows the heterogeneity of the clay surfaces, *i.e.* not all of the cation-exchange sites have the same affinity for the organic cations, which tend to occupy the most easily accessed sites first. For the additional sorption reactions of HDTMA cations, however, the heterogeneity of the clay surface sites may be overcome more or less by the increasing contributions of the chain-chain interaction of surfactants.

A probable mechanism for HDTMA molecule adsorption in smectite is shown in Figure 10. The illustration demonstrates the relationship between HDTMA adsorption and the structure of the adsorption layer influenced by the charge distribution of the clay surface. Initially (<0.7 CEC), HDTMA adsorption nearly takes place by cation exchange (Zhang *et al.*, 1993). As the HDTMA loading approaches the CEC of smectite, the selective intercalation of HDTMA develops along the silicate layers, causing the non-uniform interlayer swelling (Figures 6 and 7). As HDTMA loading increases beyond the CEC of the smectite, HDTMA adsorption may predominantly occur via hydrophobic bonding, increasing interlayer spacings to ~40 Å (Figure 10d). Although the detailed mechanism for hydrophobic adsorption of ionic surfactants is not fully known (Cases and Villieras, 1992; Bohmer and Koopal, 1992; Xu and Boyd, 1995), it is generally accepted that this process is driven by the mutual attraction between the hydrophobic alkyl chains and the tendency of the hydrophobic moieties to minimize contact with water. The limiting factor for this behavior is the repulsion arising from the charged head groups of the non-electrostatically sorbed surfactant molecules (Bohmer and Koopal, 1992). However, the binding of counterions (*e.g.* Br^-) will help to reduce the head-group repulsion (Chen *et al.*, 1992). Thus there are no restrictions to prevent additional surfactant molecules from being incorporated into the interlayers, and these could increase the interlayer spacings to 40 Å at higher HDTMA concentrations (Figures 2a, 10d). Interestingly, the cationic molecules adsorbed on the clay in excess of the CEC were not easily removed with water (Figure 3). It would seem that the binding energy of the excess quaternary cations is great due to ion-dipole and ion-ion interactions in addition to the van der Waals forces.

From the above results, it is expected that if quaternary ammonium cations, injected underground to create a sorptive zone that would immobilize organic contaminants, were adsorbed on clays at a range of concentrations, several organo-modified clay structures (*e.g.* various configurations of organic cations) can occur, influencing the partitioning of organic pollutants. If the sorbed surfactant structure changes significantly with the extent of surfactant coverage (*e.g.* if the overall sorbed surfactant packing density or order changes), then the sorptive capacity of the surfactant-modified clay for organic pollutants may change concomitantly.

CONCLUSIONS

The characteristics of cationic surfactant adsorption by swelling-layer silicates are highly complex, and the complexity arises from the structure of the adsorption layer. At low HDTMA loadings, there is a heterogeneous HDTMA/inorganic cation distribution in the interlayers and a wavy adsorption layer structure. Lateral interactions between alkyl C-16 groups of HDTMA are minimal. As HDTMA loadings increase, the contact between adsorbed HDTMA molecules increases. Selective adsorption of HDTMA into the layers of smectite results in various layer spacings at low HDTMA loadings which then become generally uniform in *d*-spacing with increasing HDTMA loading. At high HDTMA loadings on swelling clays, HDTMA adsorption via cation exchange approaches its maximum, and HDTMA adsorption via hydrophobic bonding predominantly gains in power, making some additional increase of interlayer spacing and external clay surface as a main sorption site for redundant surfactants.

REFERENCES

Ahn, J.H. and Peacor, D.R. (1986) Transmission electron microscope data for rectorite: implications for the origin and structure of 'fundamental particles'. *Clays and Clay Minerals*, **34**, 180–186.

Banfield, J.F. and Eggleton, R.A. (1988) Transmission electron microscope study of biotite weathering. *Clays and Clay Minerals*, **36**, 47–60.

Bohmer, M.R. and Koopal, L.K. (1992) Adsorption of ionic surfactants on variable-charge surfaces. 1. Charge effects and structure of the adsorbed layer. *Langmuir*, **8**, 2649–2659.

Boyd, S.A., Mortland, M.M. and Chiou, C.T. (1988) Sorption characteristics of organic compounds on hexadecyltrimethyl-ammonium-smectite. *Soil Science Society of America Journal*, **52**, 652–657.

Brindley, G.W. and Hoffmann, R.W. (1962) Orientation and packing of aliphatic chain molecules on montmorillonite. *Clays and Clay Minerals*, **9**, 546–556.

Brixie, J.M. and Boyd, S.A. (1994) Treatment of contaminated soils with organoclays to reduce leachable pentachlorophenol. *Journal of Environmental Quality*, **23**, 1283–1289.

Cases, J.M. and Villieras, F. (1992) Thermodynamic model of ionic and nonionic surfactant adsorption-abstraction on heterogeneous surfaces. *Langmuir*, **8**, 1251–1264.

Cetin, K. and Huff, W.D. (1995) Characterization of untreated and alkylammonium ion exchanged illite/smectite by high resolution transmission electron microscopy. *Clays and Clay Minerals*, **43**, 337–345.

Chen, Y.L., Chen, S., Frank, C. and Israelachvili, J. (1992) Molecular mechanisms and kinetics during the self-assembly of surfactant layers. *Journal of Colloid and Interface*

Science, **153**, 244−265.

Guthrie, G.D. and Veblen, D.R. (1990) Interpreting one-dimensional high-resolution transmission electron micrographs of sheet silicates by computer simulation. *American Mineralogist*, **75**, 276−288.

Hendershot, W.H. and Duquette, M. (1986) A simple barium chloride method for determining cation exchange capacity and exchangeable cations. *Soil Science Society of America Journal*, **50**, 605−608.

Israelachvili, J.N. (1991) *Intermolecular and Surface Forces,* 2nd edition. Academic Press, San Diego, California, 450 pp.

Lagaly, G. and Weiss, A. (1969) Determination of the layer charge in mica-type layer silicates. *Proceedings of the International Clay Conference, Tokyo* (L. Heller, editor). Israel University Press, Jerusalem, 61−80.

Lagaly, G. (1994) Layer charge determination by alkylammonium ions. Pp. 2−46 in: *Layer Charge Characteristics of 2:1 Silicate Clay Minerals* (A.R. Mermut, editor). The Clay Minerals Society, Boulder, Colorado.

Laird, D.A. (1994) Evaluation of the structural formula and alkylammonium methods of determining layer charge. Pp. 80−103 in: *Layer Charge Characteristics of 2:1 Silicate Clay Minerals* (A.R. Mermut, editor). The Clay Minerals Society, Boulder, Colorado.

Lee, J.F., Crum, J. and Boyd, S.A. (1989) Enhanced retention of organic contaminants by soils exchanged with organic cations. *Environmental Science and Technology*, **23**, 1365−1372.

Lee, J.H. and Peacor, D.R. (1986) Expansion of smectite by laurylamine hydrochloride: ambiguities in transmission electron microscope observations. *Clays and Clay Minerals*, **34**, 69−73.

Li, Z. and Bowman, R.S. (1997) Counterion effects on the sorption of cationic surfactant and chromate on natural clinoptilolite. *Environmental Science and Technology*, **31**, 2407−2412.

Marcks, C.H., Wachsmuth, H. and Reichenbach, H.V. (1989) Preparation of vermiculites for HRTEM. *Clay Minerals*, **24**, 23−32.

Mortland, M.M., Shaobai, S. and Boyd, S.A. (1986) Clay-organic complexes as adsorbents for phenol chlorophenols. *Clays and Clay Minerals*, **34**, 581−585.

Rosen, M.J. (1989) *Surfactants and Interfacial Phenomena.* John Wiley & Sons, New York, 431 pp.

Smith, J.A., Jaffe, P.R. and Chiou, C.T. (1990) Effect of ten quaternary ammonium cations on tetrachloromethane sorption to clay from water. *Environmental Science and Technology*, **24**, 1167−1172.

Theng, B.K.G. (1974) *The Chemistry of Clay-Organic Reactions.* Adam Hilger, London, 343 pp.

Vali, H. and Köster, H.M. (1986) Expanding behaviour, structural disorder, regular and random irregular interstratification of 2:1 layer-silicates studied by high-resolution images of transmission electron microscopy. *Clay Minerals*, **21**, 827−859.

Xu, S. and Boyd, S.A. (1995) Cationic surfactant adsorption by swelling and non-swelling layer silicates. *Langmuir*, **11**, 2508−2514.

Zhang, Z.Z., Sparks, D.L. and Scrivner, N.C. (1993) Sorption and desorption of quaternary amine cations on clays. *Environmental Science and Technology*, **27**, 1625−1631.